Performance Analysis of MPSK Systems in the Presence of Noisy Phase over Fading Channels

Pedro E. Gória Silva, Rausley A. A. de Souza, Daniel B. da Costa, Jules M. Moualeu, and Michel Daoud Yacoub

***Abstract*— In this paper, the performance of M-ary phase-shift keying (MPSK) modulation with imperfect carrier phase recovery over α-κ-μ and α-η-μ fading channels is investigated, for which noisy phase, assumed to be Tikhonov distributed, is considered. Analytical expressions for the exact average symbol error probability (ASEP) as well as their corresponding asymptotes for high signal-to-noise ratio (SNR) values are obtained. The derived expressions are valid for *arbitrary* values of the fading parameters, namely α, η, κ and μ, and they are validated through Monte Carlo simulations. Insightful discussions concerning the system performance as a function of the channel parameters, loop SNR, and over a wide range of SNR are drawn.**

***Keywords*— α-η-μ and α-κ-μ fading models, symbol error probability, noisy phase, Tikhonov distribution, von Mises distribution.**

I. Introduction

In wireless communication systems, the symbol error probability (SEP) performance of modulation schemes is usually addressed under the idealized hypothesis that a perfect phase reference is available at the receiver side end, i.e., an ideal coherent detection [1, Section 3.1]. In practice, this ideal scenario is never met because this local phase reference is usually extracted from a version of the transmitted signal, which inherently conveys the natural random perturbations induced by the channel, such as thermal noise, fading, and Doppler shift [1, Section 3.2]. As a result, regardless of the method used, in practice, a mismatch between the phase of the received carrier and that of the locally generated carrier exists, leading to an unavoidable phase error. The SEP of M-ary phase-shift keying (MPSK) scheme is particularly sensitive to phase error and it is more critical for high-order MPSK [1]. An approach applied to phase synchronization is the transmission of a pilot tone implemented as an unmodulated carrier, which is used directly in the synchronization process, along with the information beam. Detection schemes based on such a transmitted reference are referred to as pilot tone-aided detection techniques. On the other hand, it is possible to extract the phase of the signal received directly from the information beam. In any case, provided a phase-locked-loop (PLL) is used, the carrier phase error recovery is generally Tikhonov (a.k.a. von Mises) distributed [1], [2].

Among the various short-term fading distributions, α-η-μ and α-κ-μ [3] arise as general, flexible, and mathematically tractable models. Roughly speaking, the α-η-μ fading model represents the small-scale variation of the fading signal in a nonlinear environment for which power imbalance, or, equivalently, correlation between its quadrature components, and multipath clusters exist. On the other hand, the α-κ-μ fading model describes a fading scenario in which the nonlinear wireless channel exhibits dominant components and multipath clusters. These models have been gaining popularity with a large number of important studies available in the existing literature (e.g. [4]–[8]). From the α-η-μ and α-κ-μ fading distributions, several widely used multipath channel models can be obtained as special cases. It includes distributions such as the two-fading-parameter distributions (κ-μ, η-μ, Beckmann (η-κ), α-μ, α-κ and α-η), the one-fading-parameter ones, namely, Nakagami-m, Rice, Hoyt, and Weibull, and nonfading-parameter ones, namely, semi-Gaussian, Rayleigh, and negative exponential. [3, Sec. VI].

The impact of the phase error under a pure additive white Gaussian noise (AWGN) channel has been explored in depth in classical textbooks (e.g., [2]). The error performance over different short term fading channels has been assessed in several works (e.g., Rayleigh, Nakagami-m [9]–[11], Rician [11], α-μ [12], and η-μ, κ-μ [13]).

This paper aims to analyze the system performance in terms of the average symbol error probability (ASEP) of MPSK partially-coherent receiver-based systems under the assumption of imperfect carrier phase recovery. In particular, it generalizes some results available in the literature. The results given here apply to wireless communications systems using MPSK under the widely accepted Tikhonov phase error model.

The remainder of the paper is structured as follows. Section II describes the error-prone channel models and the phase error modeling. Section III focuses on the analysis of the exact and asymptotic ASEP for MPSK-based systems under the assumption of Tikhonov error phase. The numerical results are shown in Section IV. Finally, Section V draws some conclusions.

Notation: In this paper, $f_X(\cdot)$ denotes probability density function (PDF) of a random variable X; $\mathbb{E}(\cdot)$ is the expectation operator; $I_\nu(\cdot)$ stands for modified Bessel function of the first kind and order ν [14, eq.(8.406)], $\Gamma(\cdot)$ is the Gamma function; ${}_1F_1(\cdot;\cdot;\cdot)$ represents the confluent hypergeometric function [14, eq. (9.210.1)]; and $G_{p,q}^{m,n}\left(\cdot \,\middle|\, \begin{matrix}\cdot\\ \cdot\end{matrix}\right)$ is the Meijer's G-function [14, 9.30].

Pedro E. G. Silva and R. A. A. de Souza are with Inatel, Santa Rita do Sapucaí, Brazil (e-mail: pedrosilva@get.inatel.br; rausley@inatel.br). M. D. Yacoub is with the Wireless Technology Laboratory (WissTek), Department of Communications, School of Electrical and Computation Engineering, State University of Campinas, DECOM/FEEC/UNICAMP, 13083-852 Campinas, SP, Brazil (michel@decom.fee.unicamp.br). D. B. da Costa is with Department of Computer Engineering, Federal University of Ceará, Sobral, CE, Brazil (e-mail: danielbcosta@ieee.org). J. M. Moualeu is with the School of Electrical and Information Engineering, University of the Witwatersrand, Johannesburg 2000, South Africa (e-mail: jules.moualeu@wits.ac.za).

II. Useful Statistics

A. The α-η-μ Fading Model

The α-η-μ distribution is a general fading distribution that can be used to represent the small-scale variations of the fading signal. The PDF of the instantaneous signal-to-noise ratio (SNR) per bit of the α-η-μ fading model is given by [3]

$$f_{\Upsilon}^{\alpha\text{-}\eta\text{-}\mu}(\gamma) = \frac{\alpha\sqrt{\pi}\mu^{\mu+\frac{1}{2}}(\eta+1)^{\mu+\frac{1}{2}}}{2(\eta-1)^{\mu-\frac{1}{2}}\hat{\gamma}\sqrt{\eta}\Gamma(\mu)}\left(\frac{\gamma}{\hat{\gamma}}\right)^{\frac{\alpha}{2}\left(\mu+\frac{1}{2}\right)-1} \times \exp\left(-\frac{\mu(\eta+1)^2}{2\eta\left(\gamma/\hat{\gamma}\right)^{-\frac{\alpha}{2}}}\right) I_{\mu-\frac{1}{2}}\left(\frac{\mu(\eta^2-1)}{2\eta\left(\gamma/\hat{\gamma}\right)^{-\frac{\alpha}{2}}}\right), \quad (1)$$

where Υ is the instantaneous SNR per bit of the received signal as a function of the faded envelope R determined as $\Upsilon \triangleq R^2E_\mathrm{b}/N_0$, with E_b/N_0 being the average energy per bit to the unilateral noise power spectral density ratio, and $\hat{\gamma}$ denoting the average SNR per bit. The parameter $\hat{\gamma}$ can be written as a function of E_b/N_0 as $\hat{\gamma} = \hat{r}^2E_\mathrm{b}/N_0$, or in a similar manner $\Upsilon = \hat{\gamma}(R/\hat{r})^2$, with $\hat{r} = \sqrt{\mathbb{E}(R^2)}$. The parameter $\alpha > 0$ describes the non-linearity of the environment, $\eta > 0$ is the scattered-wave power ratio between the in-phase and quadrature components of each cluster of multipath and the total power of the scattered waves, and the shape parameter $\mu > 0$ is related to the number of multipath waves.

B. The α-κ-μ Fading Model

The α-κ-μ distribution is a general distribution that is capable of representing a line-of-sight (LoS) fading scenario under multipath components and a non-linear environment. The α-κ-μ PDF of the instantaneous SNR per bit can be written as [3]

$$f_{\Upsilon}^{\alpha\text{-}\kappa\text{-}\mu}(\gamma) = \frac{\alpha\mu(\kappa+1)^{\frac{\mu+1}{2}}}{2\kappa^{\frac{\mu-1}{2}}\hat{\gamma}\exp(-\mu\kappa)}\left(\frac{\gamma}{\hat{\gamma}}\right)^{\frac{\alpha(\mu+1)}{4}-1} \times \exp\left(\frac{\mu(\kappa+1)}{\hat{\gamma}^{\frac{\alpha}{2}}}\gamma^{\frac{\alpha}{2}}\right) I_{\mu-1}\left(\frac{2\sqrt{\kappa(\kappa+1)}\mu}{\hat{\gamma}^{\frac{\alpha}{4}}}\gamma^{\frac{\alpha}{4}}\right), \quad (2)$$

where the scale parameter $\kappa > 0$ is the ratio between the total power of the dominant components, and the parameters α and μ have been previously defined.

The number of distributions obtainable from the α-η-μ and α-κ-μ models as particular cases is enormous. An explanation for the known special cases and also the detailed meaning of each parameter can be found in [3].

C. Phase Error Modeling

For the problem at hand, we assume that the phase error Φ is Tikhonov distributed, whose PDF can be written as [2, eq. (4.35)]

$$f_\Phi(\phi) = \frac{\exp(\rho\cos\phi)}{2\pi I_0(\rho)}, \; -\pi < \phi \leq \pi. \quad (3)$$

The parameter ρ is called the loop SNR, i.e., the SNR in the bandwidth of the PLL [2], which is inversely proportional to the phase error variance [2, eq. (2.54)], i.e.

$$\sigma_\Phi^2 = \frac{1}{\rho}. \quad (4)$$

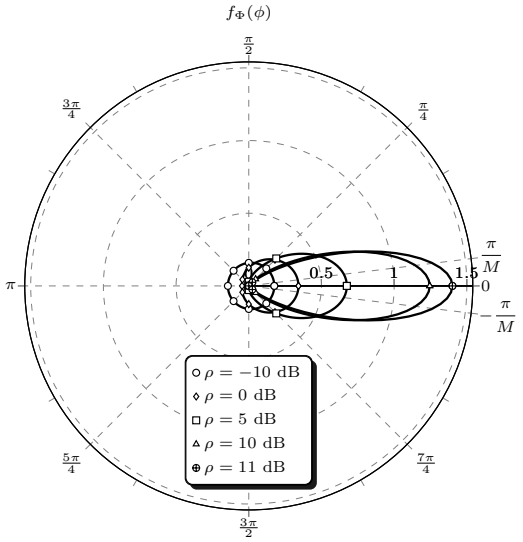

Fig. 1. The Tikhonov PDF for different values of the loop SNR ρ.

Assuming the pilot tone method, we have $\rho = P/(N_0B)$ [2, eq. (4.36)], with P representing the power of the unmodulated carrier, B is the single-sided bandwidth of the loop and N_0 is the unilateral thermal noise power spectral density. Fig. 1 shows some plots of the Tikhonov PDF, plotted in polar coordinates. Notice that when $\rho \to -\infty$ dB, (3) particularizes to a uniform distribution, leading to a circle in Fig. 1, which represents the scenario of reception without any phase synchronization. When $\rho \to \infty$, (3) tends to become an impulse (phase error PDF becomes more concentrated around $\phi = 0$ in Fig. 1), representing an ideal coherent detection. The Tikhonov PDF of (3) can be approximated by a Gaussian PDF if one makes the assumption of large loop SNR, i.e., $\rho \ggg 1$ [15]. In this case, $\rho \cong 1/\sigma^2$.

III. Performance Analysis

A. Exact ASEP under Fading Channels

With the aim of evaluating the performance of MPSK systems under AWGN, flat-slow fading channel, and imperfect carrier phase recovery impairments, the conditional symbol error probability under AWGN and noisy phase, assuming equal probable symbols, can be found as [13, eq. (9)]

$$P_\mathrm{s}(\gamma) = \frac{M-1}{M} - \frac{2}{\sqrt{\pi}I_0(\rho)}\sum_{j=1}^{\infty}\frac{I_j(\rho)\sin(j\pi/M)}{j\Gamma(j/2+1/2)2^j} \times(\gamma\log_2 M)^{j/2}{}_1F_1\left(\frac{j}{2}; j+1; -\gamma\log_2 M\right). \quad (5)$$

With the aid of [14, eq. (9.34.8)], we can replace the confluent hypergeometric function in (5) by a Meijer's G-function, to get

$$P_\mathrm{s}(\gamma) = \frac{M-1}{M} - \frac{2}{\sqrt{\pi}I_0(\rho)}\sum_{j=1}^{\infty}\frac{I_j(\rho)\sin(j\pi/M)}{j\Gamma(j/2+1/2)2^j}\frac{\Gamma(j+1)}{\Gamma(j/2)} \times(\gamma\log_2 M)^{j/2}G_{1,2}^{1,1}\left(\gamma\log_2 M\,\middle|\,\begin{matrix}1-j/2\\0,-j\end{matrix}\right). \quad (6)$$

To tie the AWGN, Tikhonov-distributed phase error and the fading channels models together, the ASEP is determined by averaging (6) over all possible values of γ, that is,

$$P_{\mathrm{s}}^{\alpha\text{-z-}\mu} = \int_0^\infty P_{\mathrm{s}}(\gamma) f_\Upsilon^{\alpha\text{-z-}\mu}(\gamma) d\gamma, \tag{7}$$

where $f_\Upsilon^{\alpha\text{-z-}\mu}(\gamma)$ is the PDF of the fading channel, with z standing for η or κ and $P_{\mathrm{s}}(\gamma)$ is the instantaneous symbol error probability as given by (6).

To evaluate the integral in (7), we first rewrite the Bessel and exponential functions in (1), for α-η-μ, or in (2), for α-κ-μ, using [14, eq. (8.445)] and [16], respectively, that is

$$I_\nu(x) = \sum_{i=0}^{\infty} \frac{(x/2)^{\nu+2i}}{i!\Gamma(i+\nu+1)} \tag{8}$$

and

$$\exp(-x) = G_{0,1}^{1,0}\left(x \,\middle|\, \begin{matrix} - \\ 0 \end{matrix}\right). \tag{9}$$

Let us define $\alpha/2 = l/b$ so that the greatest common divisor (GCD) $\mathrm{GCD}(l;b) = 1$ with l and b integer. Therefore, with the aid of [17], the exact ASEP is found as (10) for the α-η-μ channel, as shown on top of the next page, and (11) for the α-κ-μ one (see the next page), with $\Delta_0(c,d) = \{(1-d)/c, (2-d)/c, ..., (c-d)/c\}$ and $\Delta_1(c,d,f,g) = \{d/c, (1+d)/c, ..., (c-1+d)/c, (1-g)/f, (2-g)/f, ..., (f-g)/f\}$. The convergence analysis of (10) and (11) will be discussed in Section IV.

B. Asymptotic ASEP

An asymptotic result of (10) and (11) for high SNR values can be obtained as follows. Consider the system operating in a regime of large values of E_{b}/N_0. In this scenario, the errors are induced only by phase rotation since both fading and thermal noise can be neglected. The phase error is given by a Tikhonov random variable whose PDF is given by (3). Then, by assuming the Tikhonov-distributed phase error, and knowing that $|\phi| < \pi/M$ will imply a correct estimation of the transmitted MPSK symbol, the asymptotic ASEP can be calculated as

$$P_{\mathrm{s}}^{\infty} = 1 - \int_{-\pi/M}^{\pi/M} f_\Phi(\phi) d\phi. \tag{12}$$

Finally, with the help of [2, eq. (4.38)] and performing the average over the Tikhonov phase error PDF gives the desired result, namely,

$$P_{\mathrm{s}}^{\infty} = \frac{M-1}{M} - 2\sum_{n=1}^{\infty} \frac{\sin(\pi n/M)\, I_n(\rho)}{n\pi I_0(\rho)}, \tag{13}$$

that applies for both fading models analyzed in this paper.

IV. Numerical Results

In this section, we present numerical results to assess the joint effect of imperfect carrier phase recovery and fading in MPSK-based systems. The theoretical results are found by using (5) for non-fading scenario, whereas (10) and (11) so are for α-η-μ and α-κ-μ fading models, respectively. Independent simulations are performed to validate the theoretical expressions. In particular, the simulations were carried out using the MATLAB software according to the models described throughout the paper. For each point, we generate at least 10^7 samples using the Monte Carlo approach. In all figures, $\hat{r} = 1$ is assumed. Accordingly, the average SNR is given by $\hat{\gamma} = E_{\mathrm{b}}/N_0$. Due to space limitations, we analyze only the quadrature phase-shift keying (QPSK) and 8-PSK based systems. The Tikhonov samples were generated according to [18]. The phase error and the underlying fading are considered to be independent processes, as commonly assumed in the technical literature [9], [11] for pilot carrier transmission independent of the information-bearing signal. This will lead to a constant loop SNR.

In all figures, as a reference curve, the case of pure AWGN with ideal coherent detection ($\rho \to \infty$) and the case of non-fading, AWGN and imperfect carrier phase recovery, are also shown for comparison purposes.

In Fig. 2, the theoretical ASEP (dashed and solid lines) and the simulations (markers), which were obtained through Monte Carlo approach, are plotted versus the average SNR per bit in the presence of Tikhonov-distributed phase noise. The simulations evidence the usefulness and correctness of the derived analytical expressions. The corresponding theoretical ASEP curves show perfect agreement with simulation results. The plots for QPSK and 8-PSK modulations reveal the degradation in the ASEP caused by the combination of system impairments, namely AWGN, fading and carrier phase error.

In Fig. 2(a), the non-linearity parameter i.e., α, varies $\alpha = 1, 2.5$ for different values of the parameter loop SNR $\rho = 10$ dB (dashed line) and $\rho = 13$ dB (solid line), for a fixed value of the scattered-wave power ratio $\eta = 0.5$ and a fixed value of the cluster parameter $\mu = 1.5$. In Fig. 2(b), the imbalanced parameter η varies as $\eta = 0.2, 0.9$, for a fixed value of the parameters $\alpha = 2$ and $\mu = 1$. In Fig. 2(c), the clustering parameter μ varies from severe fading conditions ($\mu = 0.6$), less severe fading conditions ($\mu = 1.2$) to non-fading scenario ($\mu \to \infty$), for fixed value parameters $\alpha = 2$ and $\eta = 0.5$. In Fig. 2(c), the non-linearity parameter varies as $\alpha = 1.2, 3$ for different values of the parameter loop SNR $\rho = 10$ dB (dashed line) and $\rho = 13$ dB (solid line), for a fixed value of the scale parameter $\kappa = 1$ and a fixed value of the cluster parameter $\mu = 1.5$. In Fig. 2(d), the scale parameter κ varies as $\kappa = 0.7, 2.4$, for a fixed value of the parameter $\alpha = 2$ and $\mu = 1.5$. In Fig. 2(e), the clustering parameter μ varies from severe fading conditions ($\mu = 0.8$), less severe fading conditions ($\mu = 2.3$) to non-fading scenario ($\mu \to \infty$), for a fixed value parameter $\alpha = 2$ and $\kappa = 1$.

It is clear from these results that the 8-PSK based system performance degradation is more severe than in the QPSK based system, and, also, the 8-PSK system is extremely more susceptible than the QPSK system under variations of the parameter ρ. We can attribute this effect to the smaller Euclidean distance between symbols in the 8-PSK system. The decisive impact of the carrier phase error, both in a thermal noise scenario and in a fading channel environment, should be noted. Most importantly, the curves show a significant increase in the error probability when the loop SNR ρ decreases, since

$$P_{\mathrm{s}}^{\alpha\text{-}\eta\text{-}\mu} = \frac{M-1}{M} - \frac{\sqrt{\alpha}(\eta+1)^{2\mu} l^{\alpha\mu-1} \left(\hat{\gamma}\log_2(M)\right)^{-\alpha\mu}}{2^{2\mu-1.5}\eta^{\mu}\mu^{-2\mu}(2\pi)^{(b+l)/2-1}\Gamma(\mu)I_0(\rho)} \sum_{i=0,j=1}^{\infty} \frac{\sin\left(\frac{\pi j}{M}\right)(j-1)!I_j(\rho)}{2^j\Gamma((j+1)/2)\Gamma(j/2)} \frac{\eta^{-2i}\left(\eta^2\mu-\mu\right)^{2i}}{2^{4i}i!\Gamma(i+\mu+1/2)}$$
$$\times \left(\frac{l}{\hat{\gamma}\log_2(M)}\right)^{\alpha i} G_{2l,b+l}^{b+l,l}\left(\frac{l^l(\eta+1)^{2b}\mu^b\hat{\gamma}^{-l}}{b^b 2^b \eta^b \log_2^l(M)} \,\middle|\, \begin{matrix}\Delta_0(l,\alpha\mu+\alpha i+j/2),\Delta_0(l,\alpha\mu+\alpha i-j/2)\\ \Delta_1(b,0,l,\alpha\mu+\alpha i+1)\end{matrix}\right) \tag{10}$$

$$P_{\mathrm{s}}^{\alpha\text{-}\kappa\text{-}\mu} = \frac{M-1}{M} - \frac{\sqrt{b}l^{\alpha\mu/2-1.5}\alpha\mu^{\mu}(\kappa+1)^{\mu}\exp(-\kappa\mu)}{\sqrt{\pi}I_0(\rho)(2\pi)^{(b+l)/2-1}\left(\hat{\gamma}\log_2(M)\right)^{\alpha\mu/2}} \sum_{i=0,j=1}^{\infty} \frac{\sin\left(\frac{\pi j}{M}\right)I_j(\rho)\Gamma(j+1)}{j2^j\Gamma(j/2)\Gamma((j+1)/2)} \frac{\left(\kappa^2+\kappa\right)^i\mu^{2i}}{i!\Gamma(i+\mu)}$$
$$\times \left(\frac{l}{\hat{\gamma}\log_2(M)}\right)^{\alpha i/2} G_{2l,b+l}^{b+l,l}\left(\frac{l^l(\kappa\mu+\mu)^b}{b^b\left(\hat{\gamma}\log_2(M)\right)^l} \,\middle|\, \begin{matrix}\Delta_0(l,(\alpha\mu+\alpha i+j)/2),\Delta_0(l,(\alpha\mu+\alpha i-j)/2)\\ \Delta_1(b,0,l,(\alpha\mu+\alpha i)/2+1)\end{matrix}\right) \tag{11}$$

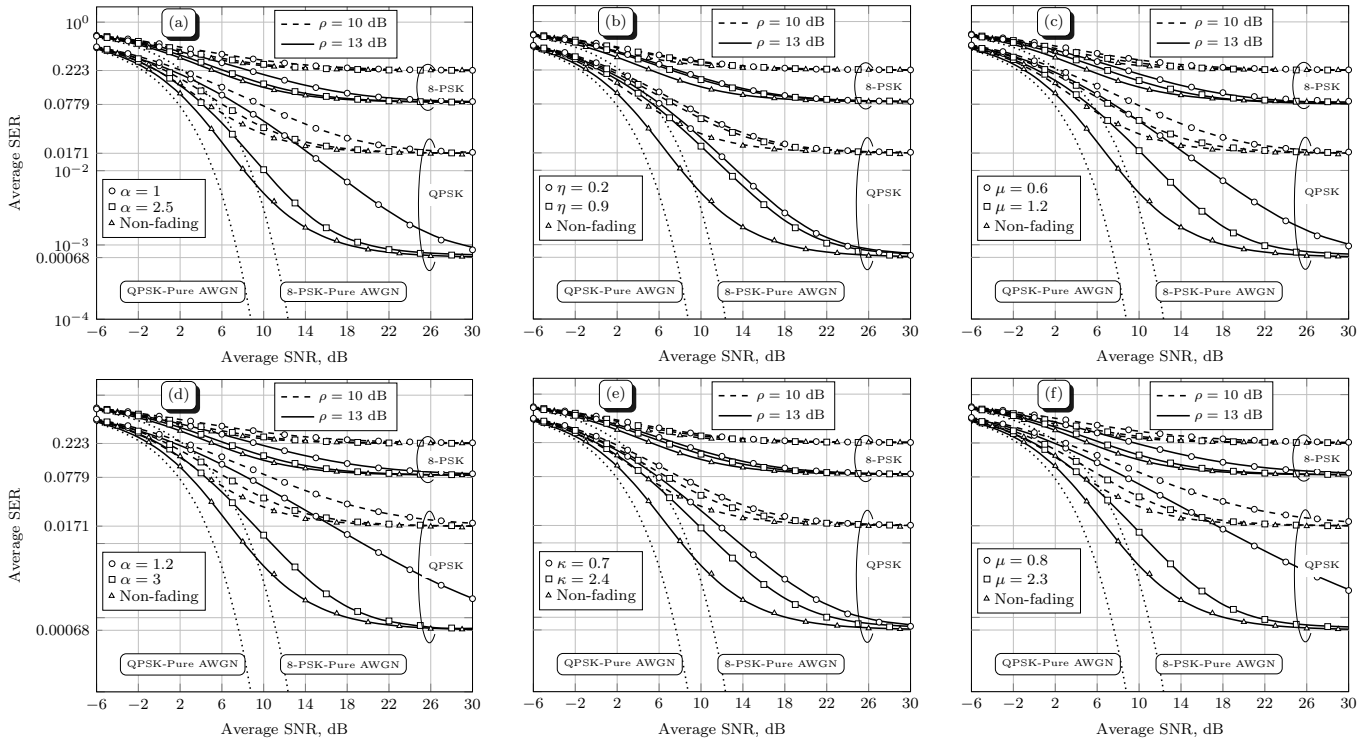

Fig. 2. ASEP versus average SNR under non-fading and α-η-μ, (a), (b) and (c), and α-κ-μ (d), (e) and (f), fading channel and Tikhonov-distributed phase error.

the variance of the Tikhonov PDF is reciprocal to the loop SNR ρ in the loop bandwidth. It is interesting to examine the behavior of the error probabilities for large SNRs. Notice that the flooring of the error rate, representing an irreducible ASEP, depends on the values of the loop SNR. Clearly, as the average SNR values tend to be higher, the thermal noise component does not alter the test statistics. Likewise, the fading component does not deteriorate the ASEP. Hence, the irreducible error probability is uniquely due to the imperfect carrier phase recovery. This irreducible error probability is in accordance with (13), which proves the correctness of our asymptotic formulations. For instance, when $\rho = 13$ dB under 8-PSK and QPSK modulations, the irreducible error probabilities are 0.0779 and 0.00068, respectively, as highlighted in the figures.

Furthermore, from Figs. 2(c) and 2(f), it is possible to conclude that the increase of the clustering parameter μ diminishes the ASEP for a fixed value of α and η or κ, respectively. From Fig. 2(b), as the imbalance parameter η increases towards 1, the performance in terms of probability of error is improved.

The ASEP expressions given in (10) or (11), although given in terms of infinite series, converges steadily and rapidly for any practical target accuracy. Fig. 3 shows the absolute error for the binary phase-shift keying (BPSK) systems versus the number of terms i and j (i.e. $i = \{0, 1, ..., K-1\}$ and $j = \{1, 2, ..., K\}$) in (10) or (11). The absolute error is calculated as the value of (10) or (11) truncated with K^2 terms in the sum minus the exact value of (7), calculated numerically. Note how the number of required terms is indeed small. For instance, the number of terms in (10) or (11) required for a seven significant

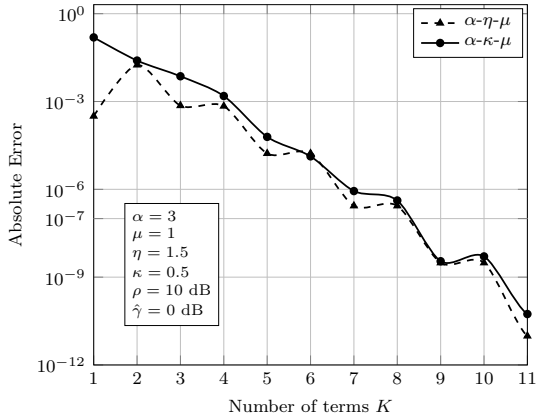

Fig. 3. Absolute error for BPSK systems versus the value of the K in each series in (10) and (11).

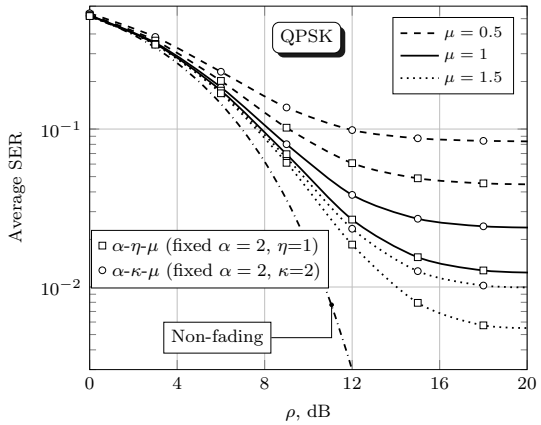

Fig. 4. ASEP against ρ for varying values of μ under α-η-μ and α-κ-μ fading channels and Tikhonov-distributed phase error under QPSK modulation.

figure accuracy is at most 8, in the evaluated scenarios.

Finally, Fig. 4 plots the ASEP of QPSK systems as a function of the loop SNR for varying values of μ under α-η-μ (fixed $\alpha = 2$ and $\eta = 1$) and α-κ-μ (fixed $\alpha = 2$ and $\kappa = 2$), and average SNR $\hat{\gamma} = 10$ dB. For small values of ρ, the ASEP tends to be high, since this is the worst scenario in terms of synchronization. Notice that, when $\alpha = 2$ and $\mu = 0.5$, $\mu = 1$, $\mu = 1.5$ for α-η-μ, the Rayleigh, the Nakagami-m ($m = 2$) and the Nakagami-m ($m = 3$) channels are obtained, and the ASEP values are in accordance with [11]. For α-κ-μ, when $\alpha = 2$ and $\mu = 1$, the Rician channel is obtained, and the ASEP values are in accordance with [11]. As the value of ρ increases, the performance improves, i.e. lower ASEP, and flooring of the error rate is achieved. This flooring, also known as symbol error floor, is now only due to the combined effects of thermal noise and fading. This flooring error probability is in accordance with [9].

V. Conclusions

We derived general, analytical expressions of the ASEP for MPSK modulation schemes in the presence of fixed phase error, AWGN, and α-η-μ or α-κ-μ fading channels. Extensive simulations have been performed to corroborate the theoretical results. Since the derived exact expressions are general, they can readily allow ASEP to assess the performance MPSK for various cases of practical interest in communication systems with phase error.

Acknowledgments

This work was supported in part by Fapemig, by CNPq (Grant 308365/2017-8, 304248/2014-2, and 302863/2017-6) and by RNP, with resources from MCTIC (Grant No. 01250.075413/2018-04), under the Radiocommunication Reference Center project of the National Institute of Telecommunications - Inatel, Brazil.

References

[1] M. K. Simon and M.-S. Alouini, *Digital communication over fading channels: a unified approach to performance analysis*, 1st ed. New York, EUA: John Wiley and Sons, 2000.

[2] A. J. Viterbi, *Principles of coherent communication*, 1st ed. New York: McGraw-Hill Book Company, 1966.

[3] G. Fraidenraich and M. D. Yacoub, "The α-η-μ and α-κ-μ fading distributions," in *2006 IEEE Ninth International Symposium on Spread Spectrum Techniques and Applications*, 2006, pp. 16–20.

[4] T. R. Rasethuntsa and S. Kumar, "An integrated performance evaluation of ED-based spectrum sensing over α-κ-μ and α-κ-μ-extreme fading channels," *Transactions on Emerging Telecommunications Technologies*, vol. 30, no. 5, p. e3569, 2019.

[5] E. Salahat and N. Yang, "Modeling recharge time of radio frequency energy harvesters in α-η-μ and α-κ-μ fading channels," in *2018 IEEE International Conference on Communications Workshops (ICC Workshops)*, 2018, pp. 1–6.

[6] M. Bhatt and S. K. Soni, "ASEP analysis over unified lognormal shadowed α-η-μ and α-κ-μ composite fading channels," in *2018 Second International Conference on Intelligent Computing and Control Systems (ICICCS)*, 2018, pp. 1126–1129.

[7] K. D. Kanellopoulou, K. P. Peppas, and P. T. Mathiopoulos, "Effective capacity analysis of equal gain diversity combiners over generalized fading channels," in *2018 IEEE 87th Vehicular Technology Conference (VTC Spring)*, 2018, pp. 1–5.

[8] J. M. Moualeu, D. B. da Costa, W. Hamouda, U. S. Dias, and R. A. A. de Souza, "Performance analysis of digital communication systems over α-κ-μ fading channels," *IEEE Commun. Lett.*, vol. 23, no. 1, pp. 192–195, 2019.

[9] A. Chandra, A. Patra, and C. Bose, "Performance analysis of PSK systems with phase error in fading channels: A survey," *Physical Communication*, pp. 63–82, Dec. 2010.

[10] C. Lo and W. Lam, "Error probability of binary phase shift keying in Nakagami-m fading channel with phase noise," *Electronics Letters*, vol. 36, no. 21, pp. 1773–1774, Oct. 2000.

[11] I. A. Falujah and V. Prabhu, "Performance analysis of PSK systems in the presence of slow fading, imperfect carrier phase recovery, and AWGN," *IEE Proc.-Commun.*, vol. 152, no. 6, pp. 903–911, Dec. 2005.

[12] P. E. G. Silva, R. A. A. de Souza, M. D. Yacoub, D. B. da Costa, and J. M. Moualeu, "Error probability of α-μ fading channels with imperfect carrier phase recovery," in *2019 IEEE 90th Vehicular Technology Conference: VTC2019-Fall*, Oct. 2019, pp. 1–5.

[13] P. E. G. Silva, R. A. A. de Souza, D. B. da Costa, J. M. Moualeu, and M. D. Yacoub, "Error probability of M-phase signaling with phase noise over fading channels," *IEEE Trans. Veh. Technol.*, vol. 69, no. 6, pp. 6766–6770, Jun. 2020.

[14] I. Grandshteyn and I. Ryzhik, *Table of integrals, series, and products*, 7th ed. New York, EUA: NY: Editora Academic Press, 2007.

[15] M. K. Simon and M.-S. Alouini, "Simplified noisy reference loss evaluation for digital communication in the presence of slow fading and carrier phase error," *IEEE Trans. Veh. Technol.*, vol. 50, no. 2, pp. 480–486, Mar. 2001.

[16] I. Wolfram Research. Meijer G-function - Exponential Function. [Online]. Available: http://functions.wolfram.com/07.34.03.0228.01

[17] I. Wolfram Research. Meijer G-function. [Online]. Available: http://functions.wolfram.com/07.34.21.0013.01

[18] D. J. Best and N. I. Fisher, "Efficient simulation of the von Mises distribution," *Journal of the Royal Statistical Society. Series C (Applied Statistics)*, vol. 28, no. 2, pp. 152–157, 1979.